Available online at www.sciencedirect.com
SCIENCE DIRECT®
Earth and Planetary Science Letters 219 (2004) 77–91
EPSL
www.elsevier.com/locate/epsl

Cenozoic marine geochemistry of thallium deduced from isotopic studies of ferromanganese crusts and pelagic sediments

Mark Rehkämper [a,*], M. Frank [a], J.R. Hein [b], A. Halliday [a]

[a] *Institute of Isotope Geology and Mineral Resources, ETH Zürich, NO C61, CH-8092 Zürich, Switzerland*
[b] *US Geological Survey, 345 Middlefield Road, Menlo Park, CA 94025, USA*

Received 21 March 2003; received in revised form 12 November 2003; accepted 26 November 2003

Abstract

Cenozoic records of Tl isotope compositions recorded by ferromanganese (Fe–Mn) crusts have been obtained. Such records are of interest because recent growth surfaces of Fe–Mn crusts display a nearly constant Tl isotope fractionation relative to seawater. The time-series data are complemented by results for bulk samples and leachates of various marine sediments. Oxic pelagic sediments and anoxic marine deposits can be distinguished by their Tl isotope compositions. Both pelagic clays and biogenic oozes are typically characterized by ε^{205}Tl greater than +2.5, whereas anoxic sediments have ε^{205}Tl of less than −1.5 (ε^{205}Tl is the deviation of the ^{205}Tl/^{203}Tl isotope ratio of a sample from NIST SRM 997 Tl in parts per 10^4). Leaching experiments indicate that the high ε^{205}Tl values of oxic sediments probably reflect authigenic Fe–Mn oxyhydroxides. Time-resolved Tl isotope compositions were obtained from six Fe–Mn crusts from the Atlantic, Indian, and Pacific oceans and a number of observations indicate that these records were not biased by diagenetic alteration. Over the last 25 Myr, the data do not show isotopic variations that significantly exceed the range of Tl isotope compositions observed for surface layers of Fe–Mn crusts distributed globally (ε^{205}Tl = +12.8 ± 1.2). This indicates that variations in deep-ocean temperature were not recorded by Tl isotopes. The results most likely reflect a constant Tl isotope composition for seawater. The growth layers of three Fe–Mn crusts that are older than 25 Ma show a systematic increase of ε^{205}Tl with decreasing age, from about +6 at 60–50 Ma to about +12 at 25 Ma. These trends are thought to be due to variations in the Tl isotope composition of seawater, which requires that the oceans of the early Cenozoic either had smaller output fluxes or received larger input fluxes of Tl with low ε^{205}Tl. Larger inputs of isotopically light Tl may have been supplied by benthic fluxes from reducing sediments, rivers, and/or volcanic emanations. Alternatively, the Tl isotope trends may reflect the increasing importance of Tl fluxes to altered ocean crust through time.

Keywords: paleoceanography; stable isotopes; isotope fractionation; seawater; ferromanganese compositions

1. Introduction

In a recent study, Rehkämper et al. [1] found that hydrogenetic ferromanganese (Fe–Mn)

* Corresponding author. Tel.: +41-1-632-7922; Fax: +41-1-632-1179.
E-mail address: markr@erdw.ethz.ch (M. Rehkämper).

0012-821X/04/$ – see front matter © 2004 Elsevier B.V. All rights reserved.
doi:10.1016/S0012-821X(03)00703-9

crusts, diagenetic Fe–Mn nodules, hydrothermal manganese deposits, and seawater have distinct Tl isotope signatures. In particular, the surface layers of hydrogenetic Fe–Mn crusts have a Tl isotope composition that differs systematically from seawater by about 2‰. In the present investigation, we extend the study of Rehkämper et al. [1] and present the first time-series Tl isotope data derived from depth profiles of Fe–Mn crusts.

Time-series of Nd, Pb, and Hf isotope compositions in Fe–Mn crusts have been used to reconstruct records of the isotopic evolution of seawater. The variations in radiogenic isotope compositions were caused either by changes in oceanic circulation patterns or by variations in the continental input fluxes to the oceans (see [2] for a recent summary). In contrast, the time-resolved O and B stable isotope data reconstructed from pelagic sediments are generally interpreted to reflect variations in factors that alter isotopic fractionation, such as ocean temperature and pH, respectively (see [3] for a recent summary).

The primary focus of the present study is to investigate whether the time-resolved Tl isotope data of serially sampled Fe–Mn crusts show variations that reflect changes in paleoceanographic conditions. To this end, we analyzed six well-characterized hydrogenetic Fe–Mn crusts that have maximum ages of between 15 and 60 Ma. In addition, we determined the Tl isotope compositions of various types of marine sediments to provide constraints on the isotopic composition of Tl sinks and thus aid in the interpretation of the Tl isotope time-series.

2. Samples

Time-resolved Tl isotope data were obtained for six hydrogenetic Fe–Mn crusts. Furthermore, we determined the Tl isotope compositions of 15 marine sediments (Fig. 1, Tables 1 and 2). All six Fe–Mn crusts were previously subjected to detailed investigations. Two samples are from the North Atlantic (Alvin 539 2-1A, water depth 2665 m; BM1969.05, 1850 m), two from the Indian Ocean (Antipode 109D-C, 5698–5178 m; DODO 232D, 4119 m) and two from the Central Pacific (F7-86-HW CD29-2, 2390–1970 m; F10-89-CP D11-1, 1870–1690 m). The Tl and Pb isotope compositions of the recent growth surfaces were measured by Rehkämper et al. [1]. Growth rates determined from Be isotopes and Co contents as well as time-series of radiogenic isotope compositions have been published previously for all these crusts [4–13] except DODO 232D. This sample has also been dated using the $^{10}Be/^{9}Be$ technique and a growth rate of 4.3 mm/Myr was determined (Frank et al., in preparation).

The three pelagic clay samples NB 23 (12°00.2′N, 138°13.0′E), NB 37 (20°00.1′N, 175°07.1′W), and NB 73 (35°14.6′N, 174°59.9′E) were collected in the West and Central Pacific Ocean at water depths of 4000–5300 m [14]. These

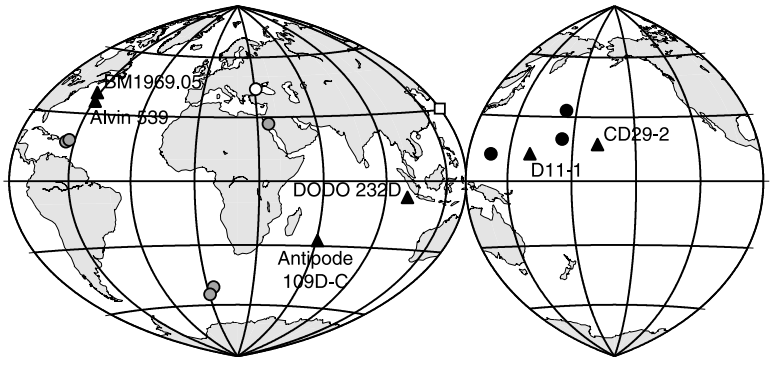

Fig. 1. Locations of the samples analyzed in the present study. Filled triangles (with labels) denote ferromanganese crusts, filled circles pelagic sediments, gray circles biogenic (carbonate and siliceous) oozes, open circles anoxic deposits, and the open square a shelf sediment.

Table 1
Tl isotope and concentration data for the sediment samples

Sample	Depth (cm)	Type	Location	Sample treatment	ε^{205}Tl	Tl (ppm)
Pelagic clays						
NB 23	core top	clay	E. Pacific	HF	3.8	0.75
NB 37	core top	clay	E. Pacific	HF	2.9	1.1
duplicate					2.6	1.2
NB 73	core top	clay	C. Pacific	HF	5.0	0.86
Biogenic sediments						
KL 80	core top	carbonate	Red Sea	6 M HCl	−0.2	0.05
M35008-3 MC	core top	carbonate	Caribbean Sea	6 M HCl	3.1	0.04
M35024-7 MC	core top	carbonate	Caribbean Sea	6 M HCl	2.4	0.09
M35024-7 MC	core top	carbonate		HF	−0.4	0.17
PS 1768-8	0–25	siliceous	S. Atlantic	6 M HCl	0.3	0.01
duplicate					0.4	0.02
PS 1768-8	0–25	siliceous		HF	−1.0	0.04
duplicate					−0.7	0.06
PS 1772-8	50–60	siliceous	S. Atlantic	6 M HCl	3.1	0.12
PS 1772-8	50–60	siliceous		HF	3.2	0.26
duplicate					3.2	0.26
PS 1772-8	320–330	siliceous	S. Atlantic	6 M HCl	7.0	0.03
PS 1772-8	320–330	siliceous		HF	5.9	0.05
Other sediments						
ECY 26	core top	clay	Yellow Sea	HF	2.3	0.21
BLS.95-2	3.5–4	calc. mud	Black Sea	HF	−2.8	0.29
BLS.95-2	5–6	calc. mud	Black Sea	HF	−2.2	0.20
BLS.95-2	19–20	calc. mud	Black Sea	HF	−2.5	0.19
USGS SDO-1	bulk	black shale		HF	−1.7	0.79
duplicate					−1.6	3.4

The duplicates represent repeat dissolutions of the sample powders. Calc.: calcareous. Sample treatment: HF digestion or 6 M HCl leaching, as described in Section 3.

samples are bulk powders from the top sections of 20–40 cm long cores. Two carbonate samples are from a 1996 Meteor cruise to the Caribbean Sea (M35008-3 MC: 18°02.5′N, 64°09.7′W, 2827 m; M35024-7 MC: 17°02.4′N, 66°00.1′W, 4701 m), and the third was collected in the Red Sea at 27°31.7′N, 34°41.2′E (909 m water depth). The siliceous oozes are from two piston cores collected in the Atlantic sector of the Southern Ocean at 52°35.6′S, 4°28.5′E (PS 1768-8) and 55°27.5′S, 1°09.8′E (PS 1772-8) [15].

Sample ECY 26 is a clay from the continental shelf of the Yellow Sea that was described by Arakaki et al. [16]. The three samples from the Black Sea are anoxic coccolith muds. They are from a core that was collected on the western continental mid-slope (43°17.1′N, 31°02.2′E) at a depth of 1536 m. The Devonian black shale SDO-1 is a USGS geological reference material.

3. Analytical methods

For the Tl isotope time-series measurements, about 5–20 mg of sample powder was typically used for analysis. Sample dissolution and chemical separation of Tl followed the techniques outlined by Rehkämper and coworkers [1,17].

About 0.2–1.5 g of sediment were either digested with HF or leached with 6 M HCl. The HF dissolution followed the silicate digestion method described by Rehkämper and Halliday [17]. For leaching, the sample powders were refluxed with 6 M HCl (~3 ml/g sample) in capped beakers for 4 h on a hotplate. After cooling, any undissolved material was separated from the solutions by centrifugation. The solutions were then evaporated to dryness and dissolved in concentrated HBr. After these initial steps, the chemical treatment of the leachates followed the HF diges-

Table 2
Tl isotope and concentration data for serially sampled ferromanganese crusts

Depth (mm)	Age (Ma)	ε^{205}Tl	Tl (ppm)
Alvin 539 2-1A			
0.5–1[a]	0.3	11.6	53
duplicate		11.8	
5	1.7	12.3	131
17	7.2	11.9	110
38	16.0	12.2	68
58–59	24.7	12.6	61
BM1969.05			
0–0.5[a]	0.2	12.3	49
0.5–1	0.5	11.5	113
1–1.5	0.8	11.4	151
1.5–2	1.1	11.4	68
duplicate		11.3	
2–2.5	1.4	11.7	72
2.5–3	1.7	11.6	86
3–3.5	2.0	11.7	100
3.5–4	2.3	12.0	86
6–7	4.0	11.3	95
9	5.6	11.3	113
13	8.0	12.1	134
22–23	13.9	14.0	114
32–33	20.1	14.8	114
48–49	29.9	14.8	87
74–75	46.0	14.8	29
103–104	50	12.4	15
106–107	52	12.2	27
112–113	53	10.7	28
117	55	9.6	44
132	59	5.3	56
duplicate		5.3	
Antipode 109D-C			
0–1[a]	0.3	13.9	73
11.5–12.5	7.7	13.2	41
37	14.0	11.4	9
duplicate		11.8	
DODO 232D			
0–1[a]	0.1	13.6	27
duplicate		13.1	
24–25	5.7	11.3	54
74–75	17.3	12.3	46
CD29-2			
0–1[a]	0.2	14.3	20
duplicate		14.2	
10.5–11	5.1	13.7	131
52–53	25.0	11.3	104
75–76	36.0	6.7	102
98	46.7	6.4	126
D11-1			
0–2[a]	0.7	14.1	91
30	14.5	12.3	96
53–54	23.2	11.8	79
60	25.6	12.1	75
77–78	32.1	10.0	151
100	40.5	9.3	59
duplicate		9.6	
129–130	51.4	6.6	86
duplicate		6.4	
135	53.4	6.9	85

All duplicates represent repeat measurements performed on the original Tl solutions obtained from the chemical separation. The ages are based on crust growth rates discussed in [9]. For DODO 232D, a ^{10}Be/^{9}Be-based growth rate of 4.3 mm/Myr was applied.
[a] Data from [1].

tion protocol (without its initial steps). The chemical separation of Tl from the sediments used the same anion-exchange chemistry that was applied to the Fe–Mn crusts, but the volume of the resin bed was increased from 100 to 300 μl. Total procedural blanks were insignificant at $<0.1\%$ of the extant Tl in the analyzed sample splits. The column chemistry was repeatedly checked during the course of this study and yields of $>95\%$ were routinely achieved. Elution experiments furthermore show that isotope fractionation of Tl during chromatographic separation is very limited [18].

The isotopic measurements followed published procedures [17,18]. All Tl isotope data were corrected for instrumental mass bias using the indigenous Pb of the samples, because this permitted the determination of Tl and Pb isotope compositions. The purified indigenous Pb was added to both the Tl sample solutions and a matching standard, containing NIST SRM 997 Tl. The mass bias correction was then conducted with the exponential law utilizing ^{208}Pb/^{206}Pb. The Tl isotope compositions of the samples are reported relative to the mean results obtained for the matching standards that were analyzed directly before and after each sample. All results are reported with an ε notation:

$$\varepsilon^{205}\mathrm{Tl} = \left(\frac{R_{\mathrm{Sample}}}{R_{\mathrm{Std}}} - 1\right) \times 10000 \qquad (1)$$

where R_{Sample} and R_{Std} denote the ^{205}Tl/^{203}Tl ratio of the sample and matching standard, respectively. A solution of Tl obtained from Aldrich

was analyzed versus the NIST SRM 997 Tl isotope standard at least once during each measurement session. The 26 analyses of Aldrich Tl, conducted over the course of about two years, yield a long-term reproducibility of ±0.38 ε^{205}Tl (2σ). Duplicate runs for the Tl sample solutions of Fe–Mn crusts, often separated by several months, always agreed in Tl isotope composition to within 0.5 ε^{205}Tl (Table 2). For duplicate dissolutions of sediments, the largest observed difference in Tl isotope composition was 0.3 ε^{205}Tl (Table 1). Laboratory experiments indicate that the accuracy of the data is similar to or slightly worse than the reproducibility at about ±0.5–0.8 ε^{205}Tl [18].

The Tl abundances were calculated from the signal intensity of ^{205}Tl during the isotopic measurements following internal standardization to ^{208}Pb. The concentration data for the Fe–Mn crusts are estimated to be precise and accurate to within about 25% [1]. The Tl abundances calculated for duplicate dissolutions of sediments do not reproduce this well for some samples (Table 1). The large differences observed for some duplicate dissolutions are probably due to either sample heterogeneity, incomplete dissolution (for some samples, e.g., SDO-1) or because Tl is lost when solutions are centrifuged to remove precipitates and undissolved residues. Following centrifugation, some solution is always lost with the solid residue, and adsorption of Tl onto precipitates may also occur. In this regard, it is noteworthy that the isotopic compositions of duplicate sediment dissolutions display excellent reproducibility for all samples (Table 1). This indicates that the isotopic results are not biased by the isotope fractionation, which may occur if Tl is lost from solutions by adsorption. The Pb isotope compositions that were acquired for the Fe–Mn crusts are not reported in this paper because the results are, with one exception (see text), identical to published data.

4. Results

4.1. Sediments

The Tl isotope compositions of the sediments are intermediate between the results obtained for the surface layers of Fe–Mn crusts and seawater (Fig. 2, Table 1). Due to the large overall variation in both ε^{205}Tl and Tl concentration, clear systematic differences between sediment types can be resolved.

The three pelagic clays display a narrow range of compositions (Fig. 2), with Tl concentrations of ~1 ppm and ε^{205}Tl of between +2.6 and +5.0. The oxic shelf sediment ECY 26 from the Yellow Sea is characterized by a Tl concentration (0.21 ppm) much lower than the pelagic clays, but its Tl isotope composition is similar with ε^{205}Tl of +2.3. The Tl isotope compositions of the calcareous and siliceous oozes vary between ε^{205}Tl values of −1 and +7 and they define a much larger field than the pelagic clays in Fig. 2, which is not simply an artifact of plotting data obtained for both HF digests and HCl leachates. The Tl concentrations of the siliceous and calcareous samples are similar

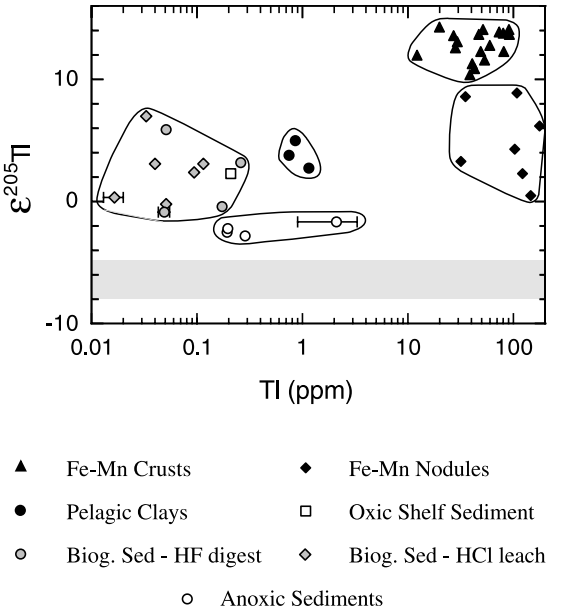

Fig. 2. Plot of ε^{205}Tl vs. Tl concentration for various marine sediments. Data are shown for recent growth surfaces of Fe–Mn crusts, diagenetic Fe–Mn nodules [1], pelagic clays, a sediment from the continental shelf of the Yellow Sea, biogenic sediments (Biog. Sed.) that were either leached with HCl or digested with HF (see text), and anoxic deposits (Table 1). The shaded area denotes the range of ε^{205}Tl (about −5 to −8) found for four seawater samples [1,18]. Error bars denote the reproducibility of duplicate dissolutions.

and, on average, lower than those observed for other sediment types with abundances of about 10–120 ppb for the HCl leachates and of 50–260 ppb for the HF digests.

The four anoxic sediments have the most seawater-like Tl isotope compositions of the sedimentary dataset with ε^{205}Tl of about −1.5 to −2.5. The three Black Sea coccolith mud samples have intermediate Tl concentrations of about 200–300 ppb, whereas the USGS black shale SDO-1 is significantly more enriched in Tl (Fig. 2, Table 1).

4.2. Depth profiles of ferromanganese crusts

For most Fe–Mn crusts, no attempt was made to obtain high-resolution depth profiles and each crust was analyzed with a resolution of 5–15 Myr (Fig. 3, Table 2). This permitted the acquisition of complete depth profiles for all samples except Alvin 539 2-1A. The oldest part of the latter sample (80–60 mm ≈ 34–25 Ma) was not analyzed.

Two sections of the crust BM1969.05 were analyzed at high resolution (Figs. 3 and 4a, Table 2). Eight samples were collected between 2.5 and 0 Ma (4–0 mm) and four samples between 55 and 50 Ma (117–103 mm). The objective was to verify whether higher-frequency variations in Tl isotope composition are superimposed on the trends that can be seen at low temporal resolution (5–15 Ma). Short-term fluctuations in Tl isotope compositions are, in principle, possible given that Tl has an oceanic residence time that is significantly shorter (∼20 kyr, Table 3) than the nominal temporal resolution of the sampling (≥300 kyr; Table 2). Both high-resolution profiles, however, display smooth trends (Figs. 3 and 4a) and all data of the 2.5–0 Ma time-series are identical, within analytical error. This suggests that Fe–Mn crusts in general do not exhibit significant short-term variations in Tl isotope composition.

Between 25 and 0 Ma, the Fe–Mn crusts do not display isotopic variations that significantly exceed the range of ε^{205}Tl values (∼+11.5 to +14.0) determined for recent growth surfaces (Figs. 3 and 4c). The only exception is crust BM1969.05, which shows an ε^{205}Tl of +14.8 between 45 and 20 Ma.

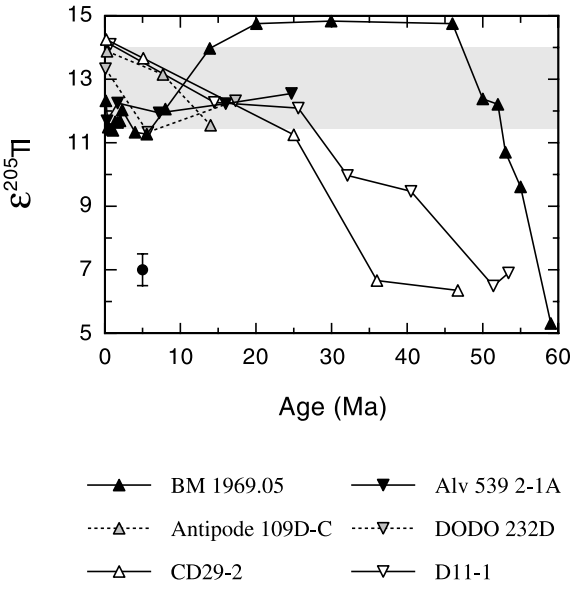

Fig. 3. Plot of Tl isotope composition (as ε^{205}Tl) vs. age (in Ma) for the six serially sampled ferromanganese crusts. The shaded area denotes the mean isotopic composition (±1σ) of the surface layers of 18 hydrogenetic Fe–Mn crust samples [1]. The estimated analytical uncertainty (±0.5 ε^{205}Tl) is shown at the left-hand bottom.

The Tl isotope compositions of the three Fe–Mn crusts with older growth layers display overall trends of increasing ε^{205}Tl with decreasing age at >25 Ma. At the base of the crusts, the samples are characterized by ε^{205}Tl values between +5 and +7, whereas values of greater than +11 are recorded at 25 Ma (Figs. 3 and 4e). Furthermore, this increase in ε^{205}Tl is nearly synchronous for the two Fe–Mn crusts from the Pacific, D11-1 and CD29-2. For the Atlantic sample BM1969.05, the timing of the increase appears to be different. As a result, the Tl isotope compositions of the Atlantic and Pacific samples differ by about 7 ε^{205}Tl at 45 Ma. It is likely, however, that this difference in timing is only due to errors in the growth rates determined for the samples. The chronology of the textually complex crust BM1969.05 is particularly uncertain, because the ^{10}Be/^{9}Be- and the Co-based chronologies do not give consistent results. Therefore, the crust sections older than 25 Ma were dated using both extrapolated ^{10}Be/^{9}Be growth rates and Co dating [9]. Cobalt dating assumes a constant hydrogenetic supply of this

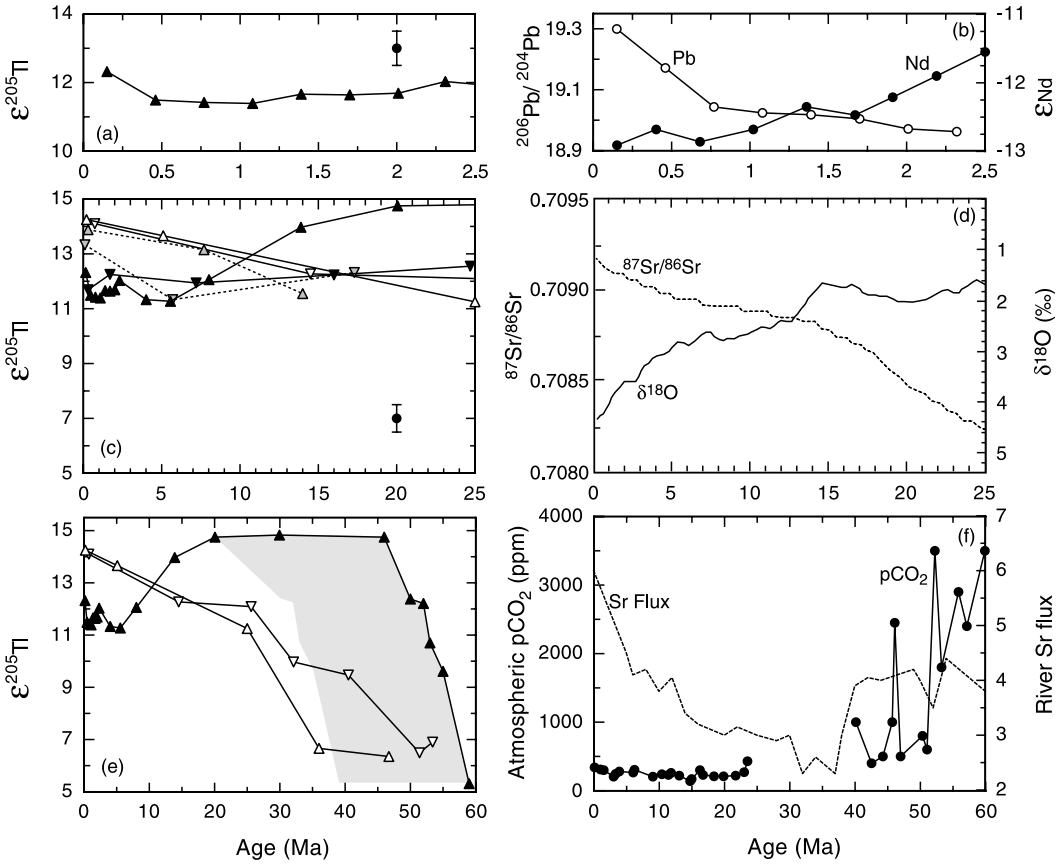

Fig. 4. Time-resolved Tl isotope data for the six serially sampled Fe–Mn crusts (symbols as in Fig. 3). Estimated analytical uncertainties of ±0.5 ε^{205}Tl are shown in panels a and c. Various published data are shown for comparison. (a) Tl isotope data for the 2.5–0 Ma high-resolution profile of sample BM1969.05. (b) Time-series of Pb [11] and Nd [8] isotope compositions for the same sample. (c) Tl isotope data for the time interval from 25 to 0 Ma. (d) Deep sea oxygen [3] and seawater Sr isotope [51] records for the same time period. (e) Tl isotope data for the three Fe–Mn crusts that have growth layers older than 25 Ma. The shaded area denotes the trends, which can be obtained for BM1969.05, assuming that ages >30 Myr may be too old by 10–20 Myr. (f) Estimate of Cenozoic atmospheric pCO_2 based on B isotopes [40]; no B and hence no pCO_2 data are available for 40–25 Ma. The riverine Sr flux (in 10^{10} mol/yr) is based on foraminiferal Sr/Ca ratios [45]; the Sr flux depends strongly on the parameters of the mass balance modeling.

element to Fe–Mn crusts, but this assumption does not appear to be valid for the North Atlantic for the entire period of the past 60 Myr. A comparison of chronologies obtained with different Co constant flux age models for BM1969.05 indicates that the ages of crust sections below 50 mm may be in error by 20 Myr or more [9]. Growth hiatuses present an additional problem, because they cannot be detected with this dating method. Assuming errors of up to 20 Myr for the oldest sections of the crust, the timing of the Tl isotope changes recorded by the Atlantic and Pacific Ocean samples at ages >25 Ma are identical, within uncertainty (Fig. 4e). Furthermore, a comparison of the Pb isotope data for CD29-2 and D11-1 with results obtained for Pacific deep-sea core L44-GPC3 suggests that these Fe–Mn crusts may have maximum ages of >65 Myr [19] and application of a chronology that is based on these older ages generates nearly synchronous Tl isotope trends for the Pacific Ocean samples and BM1969.05.

It is also noted that the measured Pb isotope composition for the base of BM1969.05 (132

mm = 59 Ma, $^{206}Pb/^{204}Pb = 19.13$) differs from results obtained for slightly younger sections of the crust (e.g., 103.5 mm, $^{206}Pb/^{204}Pb = 18.83$) in this and previous studies [4]. The Tl isotope composition at 132 mm, however, lies at the extension of a clear trend defined by the five previous samples (103–117 mm, Fig. 3), which demonstrates that the base of the crust is not a recent overgrowth.

5. Discussion

5.1. Tl isotope composition of Fe–Mn crust growth surfaces: implications for fractionation mechanisms

In a previous study Rehkämper et al. [1] demonstrated that the surface layers of hydrogenetic Fe–Mn crusts are characterized by a global signature of $\varepsilon^{205}Tl = +12.8 \pm 1.2$ (1σ). In contrast, three seawater measurements yielded a significantly lighter isotope composition of $\varepsilon^{205}Tl \approx -6$. Two distinct mechanisms could be responsible for the large difference in Tl isotope compositions between seawater and Fe–Mn crusts and account for the observed fractionation factor of $\alpha_{Sw-Cr} \approx 1.0019$. Rehkämper et al. [1] proposed that the isotope fractionation results from the adsorption of Tl onto the surfaces of Fe–Mn oxide particles. Alternatively, the isotopic difference may reflect isotope fractionation of Tl in seawater, for example between the two redox states of thallium, Tl(I) and Tl(III).

Thermodynamic calculations and other observations indicate that Tl should occur primarily as Tl(I) in seawater (see [20] for a summary). If there is isotope fractionation between dissolved Tl(I) and Tl(III), mass balance requires the minor species (Tl^{3+}) to be enriched in ^{205}Tl. Therefore, preferential adsorption of Tl(III) characterized by high $\varepsilon^{205}Tl$ would need to be responsible for the heavy Tl isotope signatures of Fe–Mn crusts. Leaching experiments, however, show that Tl is associated primarily with the Mn-oxide phases of Fe–Mn crusts [21]. This indicates that Tl is scavenged as a monovalent cation from seawater, because Tl^{3+} would be preferentially adsorbed by Fe-oxides. Therefore, the Tl isotope compositions of the Fe–Mn crusts are unlikely to reflect preferential adsorption of the isotopically heavy Tl(III) species. It is also possible, however, that isotope fractionation occurs between different dissolved Tl(I) species, one of which is preferentially adsorbed. Similar models have been proposed previously to explain various Fe isotope effects [22,23].

Alternatively, it is possible that the heavy Tl isotope compositions of Fe–Mn crusts are generated by the adsorption of Tl^{+} from seawater onto Fe–Mn oxides and/or the subsequent surface oxidation of Tl^{+} to Tl^{3+} [1]. This model accounts for the nearly constant isotopic offset between the growth surfaces of Fe–Mn crusts and seawater by the equilibrium isotope fractionation that would result, for example, from the stronger bonding of ^{205}Tl compared to ^{203}Tl. It is notable that such surface adsorption processes are known to produce large isotopic fractionations for other elements in natural systems (e.g., [24]) and experimental studies [25] indicate they are responsible for the fractionated Mo isotope signatures of Fe–Mn deposits relative to seawater.

In the absence of experimental studies, which provide constraints on the origin of the fractionated Tl isotope compositions of the Fe–Mn crusts, we favor the adsorption mechanism as the most viable working hypothesis because this provides a comprehensive and yet straightforward explanation for all observations. This model accounts not only for the constant Tl isotope compositions of the Fe–Mn crust surfaces, but also for the variable $\varepsilon^{205}Tl$ values of Fe–Mn nodules [1] and pelagic clays (see below). In addition, this interpretation implies that the Tl isotope composition of the present oceans should be constant to within about ± 1.5 $\varepsilon^{205}Tl$. The limited Tl isotope data presently available for seawater [1,18] are in accord with this conclusion, but further analyses are desirable to verify this result. The conclusion is also in agreement with the ~20 kyr marine residence time of Tl (Table 3). With a residence time that is significantly longer than the mixing time of the oceans (about 1 kyr) and a nearly conservative distribution [20], significant Tl isotope variations are not expected in seawater.

Table 3
Source and sink fluxes of dissolved marine Tl and oceanic residence times calculated from these values [20]

	Tl flux	
	Range	Best estimate
Input fluxes		
Rivers	0.8–1.9	1.3
Hydrothermal fluids	0.3–2.7	1.2
Subaerial volcanism	0.2–4.3	1.6
Mineral aerosols	0.1–1.0	0.4
Benthic fluxes from continental margins	0.03–2.0	0.7
Total	1.4–12	5.2
Residence time	7–63 kyr	17 kyr
Output fluxes		
Pelagic clays	1.0–2.0	1.3
Altered oceanic crust	0.6–5.7	2.9
Total	1.6–7.7	4.2
Residence time	11–56 kyr	21 kyr

All fluxes are given in units of Mmol/yr. The residence times are calculated for an oceanic Tl inventory of 8.76×10^4 Mmol [20]. The range of flux values reflects the uncertainties of the estimates.

5.2. Tl isotopes in sediments

Although the database is still limited, there appears to be a systematic difference in Tl isotope compositions between oxic and anoxic sediments (Fig. 2). The four anoxic sediments are characterized by ε^{205}Tl of less than −1.5, whereas most oxic pelagic sediments have ε^{205}Tl of greater than +2.4. In terms of their Tl isotope composition, oxic pelagic sediments are thus similar to diagenetic Fe–Mn nodules and the recent growth surfaces of Fe–Mn crusts, whereas anoxic sediments display only minor fractionation relative to seawater (Fig. 2). It is noteworthy that the Tl isotope systematics of the sediments are strikingly similar to the sediment variations of the Mo isotope system, the main difference being the opposite sign of the isotope fractionation [26,27].

It is reasonable to assume that the positive ε^{205}Tl values of oxic pelagic sediments and Fe–Mn crusts ultimately have the same or a similar origin, and this was inferred to be the preferential adsorption of ^{205}Tl. This fractionation model, however, requires an explanation for the observation that oxic pelagic sediments have lower and more variable ε^{205}Tl than the recent growth surfaces of Fe–Mn crusts. Two factors may be responsible. First, it is notable that oxic sediments and diagenetic Fe–Mn nodules display a similar range of Tl isotope compositions (Fig. 2). Therefore, it is possible that ε^{205}Tl in sediments is, at least in part, controlled by the uptake of Tl from pore fluids, which can act as a closed-system reservoir that limits the isotope fractionation during adsorption [1]. Second, oxic pelagic sediments derive only part of their Tl budget from authigenic oxyhydroxides. Significant additional Tl is present in the lattices or bound loosely to the surfaces of clays [28] and other detrital minerals, and this Tl appears to be characterized by $\varepsilon^{205}\mathrm{Tl} < 0$.

The latter explanation is supported by the results obtained for biogenic sediments that were analyzed by both total (HF) dissolution and HCl leaching (Table 1). The leaching procedure should dissolve quantitatively authigenic Fe–Mn oxyhydroxides. Carbonates will also be dissolved, however, and the leach is probably sufficiently harsh to release some of the Tl associated with detrital phases and biogenic opal. Because biogenic carbonate and silica are unlikely to have high Tl contents [20,29,30], the data provide a rough estimate of the Tl signals contributed by authigenic and detrital phases. A better chemical separation of these signals would require a more selective leaching technique and this may generate isotopic fractionation. The simple leaching procedure adopted here avoids this problem, as is clearly shown by the excellent reproducibility of

the isotope data for duplicate dissolutions (Table 1). The comparison of HF dissolution and HCl leachate data shows that only about 50% of the Tl in biogenic sediments is released by leaching, such that a significant fraction is locked up in more resistant (detrital) phases. With one exception, the leached Tl has a significantly heavier isotope composition than the HF digests (Table 1). This indicates that the authigenic phases of pelagic sediments are responsible for generating positive overall ε^{205}Tl, whereas the detrital Tl typically has $\varepsilon^{205}\mathrm{Tl} < 0$.

Authigenic oxyhydroxides are not formed in anoxic environments and their absence can explain the negative ε^{205}Tl values of anoxic sediments. In anoxic sediments, the Tl is associated either with detrital phases (which are inferred to have low ε^{205}Tl) or sulfides, which can have high Tl abundances [31]. The high Tl concentrations of black shales [30] indicate that sulfides may indeed be an important Tl carrier phase in anoxic environments. The isotope data obtained for SDO-1 (Table 1), which contains 5.4% S, then suggest that little or no isotope fractionation occurs when Tl is coprecipitated from solution with sulfides.

5.3. Tl isotope time-series of ferromanganese crusts

5.3.1. Do the trends reflect alteration or are they primary?

It is possible that the Tl isotope time-series data are biased by diagenetic effects, but there are a number of observations that argue against this interpretation. First, all six Fe–Mn crusts show similar Tl isotope trends from 25 to 0 Ma, with Tl isotope compositions that do not significantly exceed the range of ε^{205}Tl values determined for recent growth surfaces. This coherency suggests that the samples record a primary paleoceanographic signal, at least in the younger (<25 Ma) growth layers. Second, this conclusion is reinforced by the observation that the two Fe–Mn crusts from the Pacific show no significant inflection in their Tl isotope evolution due to diagenetic phosphatization. The older (>20 Ma) growth layers of most Pacific Ocean crusts from water depths above 2500 m have been affected by several episodes of phosphogenesis, which generated the most obvious diagenetic signatures recorded in the crusts [32,33]. Phosphatization is recorded by CD29-2 and D11-1 in growth layers older than 25 and 18.5 Ma, respectively [6]. The absence of distinct changes in the Tl isotope time-series of these samples between 25 and 15 Ma (Figs. 3 and 4c,e) indicates that phosphatization did not reset or significantly alter the primary Tl isotope signals. Third, Tl isotopes should show approximately the same resistance to post-depositional exchange with seawater as Nd, Pb, Hf, or Mo according to the empirical relationships presented by Henderson and Burton [34], and the isotope compositions of the latter elements are interpreted to be primary in Fe–Mn crusts even at >25 Ma [9,26]. Fourth, modification of ε^{205}Tl in older crust sections (>25 Ma) by reaction with seawater should generate heavy Tl isotope compositions, similar to those found in recent growth layers. This would serve to erase the relatively low ε^{205}Tl values of these layers and obscure the observed secular variations in ε^{205}Tl. Fifth, diagenesis or diffusion should erase differences or gradients in Tl concentrations along the Fe–Mn crust depth profiles. Most samples, however, display significant variations in Tl abundances (Table 2). Sixth, it could be envisioned that the Tl isotope trends at >25 Ma may be due to the incorporation of Tl derived from substrate rocks or from sediment. In this scenario, however, all Fe–Mn crusts should display ε^{205}Tl of about +6 at the base, but such values are only observed at the base of crusts older than 35 Ma. Furthermore, it has been shown that substrate rocks do not contribute to crust compositions [35]. Taken together, these observations build a strong case against the interpretation that the Tl isotope time-series data reflect diagenetic alteration.

5.3.2. Tl isotopes in the 25–0 Ma growth layers

The constancy of ε^{205}Tl in the 25–0 Ma growth layer of the Fe–Mn crusts (Fig. 4a,c) contrasts with other marine isotope records that display marked changes during the same time period. The 2.5–0 Ma profile of BM1969.05 is important in this respect, because the Pb, Nd, and Hf isotope compositions display large variations (Fig.

4b) that are thought to be due to changes either in the amount of continental input into the North Atlantic or in the weathering regime in northern Canada and Greenland [7,9,12,13]. The Tl isotope compositions are constant and thus unperturbed by the processes that drove variations in radiogenic isotope compositions (Fig. 4a). This conclusion is supported by the Tl isotope time-series data in general, which display no significant correlations with published Pb, Nd, or Hf isotope depth profiles for any of the Fe–Mn crusts. It is possible, however, that this lack of correlation simply reflects the longer oceanic residence time of Tl ($\tau \approx 20$ kyr; Table 3) compared to Pb, Nd, and Hf ($\tau \leq$ about 2 kyr [2]).

Marine sediments furthermore record large variations in the Os and Sr (Fig. 4d) isotope compositions of seawater for the last 25 Myr. Compared to Tl, Sr and Os have marine residence times that are comparable ($\tau_{Os} \approx 10$–50 kyr [36]) or longer ($\tau_{Sr} \approx 4$ Myr [37]), respectively. During the last 25 Myr, $^{87}Sr/^{86}Sr$ and $^{187}Os/^{188}Os$ have become increasingly radiogenic and these variations are interpreted to reflect larger riverine fluxes of these elements and/or riverine fluxes that have become more radiogenic through time [36,38]. The fact that the Sr and Os isotope compositions of seawater changed considerably during the last 25 Myr, whereas Tl isotopes did not, indicates that these isotope systems are decoupled in the marine environment. Such a decoupling is not surprising given that variations in radiogenic isotope compositions for continent-derived fluxes reflect differences in parent/daughter ratios and ages of the source rocks. These factors have no impact on Tl isotope compositions, which makes it reasonable to assume that the continental crust is relatively homogeneous in ε^{205}Tl.

In addition, it is noteworthy that the stable oxygen isotope compositions of benthic foraminifera show a marked shift toward more positive $\delta^{18}O$ values during the last 25 Myr, which reflects, besides an ice volume effect, a decline in ocean bottom-water temperatures [3]. Recent Cenozoic records of benthic foraminiferal Mg/Ca suggests that bottom-water temperatures decreased by about 5–6°C from 25 Ma to the present [39]. The absence of a global Tl isotope trend during this time period therefore indicates that the Tl isotope signatures of Fe–Mn crusts are not significantly altered by small (5°C) changes in ocean temperatures.

5.3.3. *Tl isotopes in the >25 Ma growth layers*

The Tl isotope compositions of the three Fe–Mn crusts with growth layers older than 25 Ma display trends of increasing ε^{205}Tl with decreasing age (Fig. 4e). Given the large uncertainties in the chronology, the timing of this increase is essentially synchronous for all samples. There are two models that can account for these observations. Either the variations are due to changes in the fractionation factor α_{Sw-Cr}, which is responsible for the heavy Tl isotope signatures of Fe–Mn crusts relative to seawater. Alternatively, they may reflect a change in the Tl isotope composition of seawater.

With regard to the first model, the constancy of ε^{205}Tl in the Fe–Mn crusts during the last 25 Myr argues strongly against the interpretation that the trends are caused by temperature-induced changes in α_{Sw-Cr}. Furthermore, there is no systematic variation in the mineralogy or major element chemistry of the crusts that could account for an increase in α_{Sw-Cr} from 60 to 25 Ma [9]. It is also possible, however, that the fractionation factor responded to variations in the adsorption mechanism or the speciation of dissolved Tl, and such variations could be induced by changes in seawater composition or pH. In this regard, it is noteworthy that the increase in ε^{205}Tl for the Fe–Mn crusts from 60 to 25 Ma is similar in timing to the decrease in ocean pH as inferred from the B isotope compositions of foraminifera [40]. The interpretation of such B isotope data in terms of ocean pH has recently been challenged [41], but nonetheless this remains a viable mechanism.

A comprehensive assessment of whether variations in α_{Sw-Cr} are responsible for the observed Tl isotope trends is not possible until the mechanism of Tl isotope fractionation between seawater and Fe–Mn particles is fully understood. The observation that the Mo stable isotope time-series for Fe–Mn crusts display uniform isotope compositions for the last 60 Myr [26], however, argues against

this interpretation. It is reasonable to assume that any change in α_{Sw-Cr} for Tl (e.g., due to a jump in ocean pH) would also affect the Mo isotope fractionation factor, but the Mo isotope time-series data [26] record no such change.

It is therefore more likely that the trends of ε^{205}Tl reflect variations in the Tl isotope composition of seawater, which are caused by changes in either the oceanic output or input fluxes of Tl. An evaluation of this interpretation requires an understanding of the sources and sinks of dissolved oceanic Tl and, in particular, their isotopic signatures. Based on a review of published data, Rehkämper and Nielsen [20] inferred that the primary sources of dissolved Tl in the oceans are rivers, hydrothermal fluids, eolian contributions from volcanic emanations and mineral aerosols, and benthic fluxes from continental margin sediments (Table 3). The two main oceanic sinks were thought to be scavenging of Tl from seawater by the authigenic phases of pelagic clays and uptake of Tl during low-temperature alteration of oceanic crust (Table 3). Thallium isotope data, however, are presently available solely for seawater and the sediments analyzed in the present study. Therefore, only a preliminary evaluation of whether the Tl isotope trends of the Fe–Mn crust time-series indeed reflect a secular change in the isotope composition of seawater is possible.

In order to generate ε^{205}Tl values for seawater that increase toward the present, the isotope composition of the total output flux must have evolved from higher to lower ε^{205}Tl values, such that the overall fractionation factor relative to seawater decreased. A shift from predominantly oxic to predominantly anoxic sedimentation could generate an appropriate change in the isotope composition of seawater, but both Mo isotope data [26] and sedimentary records [42] argue against this interpretation. Alternatively, this change could be produced by larger output fluxes of Tl to altered ocean crust if this flux is characterized by an average isotope composition with ε^{205}Tl of less than ~ 0.

If the increase of ε^{205}Tl for seawater was generated by variations in the oceanic input fluxes of Tl, this requires sources at ~ 60 Ma that delivered isotopically light Tl to the oceans, and the importance of these sources must have decreased with time. Alternatively, the role of source fluxes with high ε^{205}Tl may have increased toward the present. The secular evolution of hydrothermal fluxes can be evaluated, to a first order, if they are assumed to scale with spreading rate. A recent inversion [43] of new area versus age data for ocean crust indicates that ridge production was constant to within about $\pm 10\%$ for the last 180 Myr. This implies that hydrothermal fluxes are unlikely to have generated the observed Tl isotope trends (Fig. 4e). A similar conclusion is also reasonable for the mineral aerosols. They constitute only a minor source of Tl at present (Table 3) and are likely to have been even less significant in the early Cenozoic [44].

The (model-dependent) Cenozoic seawater Sr/Ca record of Lear et al. [45] suggests that riverine Sr fluxes may have decreased by about 40% between 60 and 30 Ma (Fig. 4f). Because this decrease was inferred to be mainly a response to lower silicate weathering rates, it should also be associated with lower river Tl fluxes. In addition, it is possible that benthic input fluxes were larger in the early Cenozoic compared to the present, because anoxic sedimentation was more widespread [42]. Either of these fluxes may have generated lower ε^{205}Tl for seawater from 60 to 25 Ma, if they delivered isotopically light Tl to the oceans.

Of particular interest is the possibility that the Tl isotope trends were generated by larger fluxes of Tl derived from subaerial volcanism. This interpretation is not unreasonable given that the increase in ε^{205}Tl from 60 to 25 Ma resembles the decrease of atmospheric CO_2 (Fig. 4f), as inferred from the paleo-pH of surface seawater (calculated from B isotopes [40]) and other data [46]. On long time scales (millions of years), variations in atmospheric CO_2 appear to be governed primarily by volcanic and metamorphic outgassing and CO_2 consumption by weathering [47]. The higher CO_2 levels deduced for the time period from 60 to 40 Ma have been related to enhanced volcanic activity, based on geological evidence, mass balance considerations, and modeling results [40,48,49]. Subaerial volcanic emanations are known to deliver large quantities of Tl into the

atmosphere (Table 3) and submarine degassing of Tl may also be important [50]. Because partial evaporation occurs when such volcanic gases are produced, the emanations should be enriched in ^{203}Tl (the light isotope) and display low ε^{205}Tl.

In summary, these results imply that larger benthic fluxes of Tl and/or increased inputs from rivers as well subaerial volcanism may have been responsible for the low ε^{205}Tl values of Fe–Mn crusts and seawater in the early Cenozoic (Fig. 4e). Previous studies indicate that the importance of these Tl fluxes probably decreased from about 60 to 30 Ma (Fig. 4f), and this could explain why Fe–Mn crusts display increasing ε^{205}Tl with decreasing age. Alternatively, the Tl isotope trends may reflect the increasing relative importance of Tl output fluxes to altered ocean crust through time.

6. Conclusions

The recent surfaces of hydrogenetic Fe–Mn crusts show a global and relatively constant signature of high ε^{205}Tl relative to seawater and very similar Tl isotope compositions are recorded in the 25–0 Ma growth layers of six Fe–Mn crusts. For three of these samples, Tl isotope data were also acquired for growth layers older than 25 Ma. These section show ε^{205}Tl increasing from about +6 at ~55 Ma to values of about +12 at 25 Ma.

The interpretation of these results is difficult at present, due to our limited understanding of the marine isotope geochemistry of Tl. All presently available data, however, are in accord with the following working hypotheses: (1) the systematic difference in Tl isotope compositions between recent Fe–Mn crust surfaces and seawater are due to the equilibrium isotope fractionation that occurs during the adsorption of Tl on Fe–Mn particles and subsequent oxidation; (2) the trends of the Tl isotope time-series reflect variations in the Tl isotope composition of seawater.

Future studies need to test these hypotheses and establish refined or revised interpretations. On the one hand, this will require laboratory experiments, which investigate the mechanism of Tl isotope fractionation between seawater and Fe–Mn crusts. Factors that potentially influence the fractionation factor need to be explored and the speciation of dissolved Tl in the oceans should be further investigated. On the other hand, the Tl isotope compositions of the main sources and sinks of dissolved oceanic Tl need to be established. In addition, it is desirable to evaluate whether the oxyhydroxide fractions of pelagic sediments also exhibit systematic variations in Tl isotope compositions. Such measurements are of particular interest because the ~20 kyr oceanic residence time of Tl is sufficiently short for climatically driven changes in the Tl isotope composition of seawater to be recorded in sediment layers that can be sampled at high temporal resolution.

Acknowledgements

We are particularly grateful to those colleagues who made samples available to us. The Pacific Ocean and the Yellow Sea clays were collected as part of the Northwest Pacific Carbon Cycle Project (NOPACC) and were provided by the Geological Survey of Japan. We received the samples from Dr. Nishimura (GSJ) and Dr. Y. Asahara (Nagoya University). Jana Friedrich, Cristian Teodoru and Bernhard Wehrli (EAWAG/ETH, Kastanienbaum, Switzerland) provided the Black Sea sediments. The carbonate oozes are from the collection of Ralf Schiebel (ETH). The biogenic siliceous sediments from the Southern Ocean were supplied by the Alfred-Wegener-Institute for Polar and Marine Research (Bremerhaven, Germany). H. Baur, D.-C. Lee, M. Maier, U. Menet, D. Niederer, S. Nielsen, F. Oberli, B. Rütsche, A. Süsli, C. Stirling, H. Williams, and S. Woodland are thanked for their help in keeping the mass spectrometers running smoothly and support in the clean labs. The paper profited immensely from discussions with S. Nielsen, D. Porcelli, R. Schiebel, D. Schmidt, and T. van de Flierdt. The constructive reviews of A. Anbar and B. Peucker-Ehrenbrink were of great help in producing a significantly improved revised version of the script. Financial support by the Schweizerische Nationalfond (SNF) is acknowledged. *[BOYLE]*

References

[1] M. Rehkämper, M. Frank, J.R. Hein, D. Porcelli, A.N. Halliday, J. Ingri, V. Liebetrau, Thallium isotope variations in seawater and hydrogenetic, diagenetic, and hydrothermal ferromanganese deposits, Earth Planet. Sci. Lett. 197 (2002) 65–81.

[2] M. Frank, Radiogenic isotopes: Tracers of past ocean circulation and erosional input, Rev. Geophys. 40 (2002) 1–38.

[3] J. Zachos, M. Pagani, L. Sloan, E. Thomas, K. Billups, Trends, rhythms, and aberrations in global climate 65 Ma to present, Science 292 (2001) 686–693.

[4] K.W. Burton, H.-F. Ling, R.K. O'Nions, Closure of the Central American Isthmus and its effect on deep-water formation in the North Atlantic, Nature 386 (1997) 382–385.

[5] J.N. Christensen, A.N. Halliday, L.V. Godfrey, J.R. Hein, D.K. Rea, Climate and ocean dynamics and the lead isotopic records in Pacific ferromanganese crusts, Science 277 (1997) 913–918.

[6] H.F. Ling, K.W. Burton, R.K. O'Nions, B.S. Kamber, F. von Blanckenburg, A.J. Gibb, J.R. Hein, Evolution of Nd and Pb isotopes in Central Pacific seawater from ferromanganese crusts, Earth Planet. Sci. Lett. 146 (1997) 1–12.

[7] R.K. O'Nions, M. Frank, F. von Blanckenburg, H.-F. Ling, Secular variations of Nd and Pb isotopes in ferromanganese crusts from the Atlantic, Indian and Pacific Oceans, Earth Planet. Sci. Lett. 155 (1998) 15–28.

[8] K.W. Burton, D.-C. Lee, J.N. Christensen, A.N. Halliday, Actual timing of neodymium isotopic variations recorded by Fe–Mn crusts in the western North Atlantic, Earth Planet. Sci. Lett. 171 (1999) 149–156.

[9] M. Frank, R.K. O'Nions, J.R. Hein, V.K. Banakar, 60 Myr records of major elements and Pb-Nd isotopes in hydrogenous ferromanganese crusts: Reconstruction of seawater paleochemistry, Geochim. Cosmochim. Acta 63 (1999) 1689–1708.

[10] D.-C. Lee, A.N. Halliday, J.R. Hein, K.W. Burton, J.N. Christensen, D. Günther, Hafnium isotope stratigraphy of ferromanganese crusts, Science 285 (1999) 1052–1054.

[11] B.C. Reynolds, M. Frank, R.K. O'Nions, Nd- and Pb-isotope time series from Atlantic ferromanganese crusts: implications for changes in provenance and paleocirculation over the last 8 Myr, Earth Planet. Sci. Lett. 173 (1999) 381–396.

[12] A.M. Piotrowski, D.-C. Lee, J.N. Christensen, K.W. Burton, A.N. Halliday, J.R. Hein, D. Günther, Changes in erosion and ocean circulation recorded in the Hf isotopic compositions of North Atlantic and Indian Ocean ferromanganese crusts, Earth Planet. Sci. Lett. 181 (2000) 315–325.

[13] T. van de Flierdt, M. Frank, D.-C. Lee, A.N. Halliday, Glacial weathering and the hafnium isotope composition of seawater, Earth Planet. Sci. Lett. 201 (2002) 639–647.

[14] M. Takebe, Rare earth element composition of deep sea sediments from central to western Pacific – Discussion about main factors controlling REE compositions of marine sediments by factor analysis, J. Geol. Soc. Japan 107 (2001) 301–315.

[15] M. Frank, R. Gersonde, M. Rutgers van der Loeff, G. Bohrmann, C. Nürnberg, P.W. Kubik, M. Suter, A. Mangini, Similar glacial and interglacial export bioproductivity in the Atlantic sector of the Southern Ocean: Multiproxy evidence and implications for atmospheric CO_2, Paleoceanography 15 (2000) 642–658.

[16] T. Arakaki, Y. Dokiya, Y. Kodama, J. Ohyama, K. Ogawa, T. Sagi, Chemical characterization of sediments from the East China Sea and the Yellow Sea, Geochem. J. 28 (1994) 31–46.

[17] M. Rehkämper, A.N. Halliday, The precise measurement of Tl isotopic compositions by MC-ICPMS: Application to the analysis of geological materials and meteorites, Geochim. Cosmochim. Acta 63 (1999) 935–944.

[18] S.G. Nielsen, M. Rehkämper, J. Baker, A.N. Halliday, The precise and accurate determination of thallium isotope compositions and concentrations for water samples by MC-ICPMS, Chem. Geol. (2004) in press.

[19] H.-F. Ling, S.-Y. Jiang, M. Frank, Y. Zhou, F. Zhou, Z.-L. Lu, P. Ni, X.-M. Chen, Differing controls over the Cenozoic Pb and Nd isotope evolution of deepwater in the central North Pacific Ocean, Earth Planet. Sci. Lett. (2004) submitted.

[20] M. Rehkämper, S.G. Nielsen, The mass balance of dissolved thallium in the oceans, Mar. Chem. (2004) in press.

[21] A. Koschinsky, J.R. Hein, Uptake of elements from seawater by ferromanganese crusts: Solid-phase associations and seawater speciation, Mar. Geol. 198 (2003) 331–351.

[22] T.D. Bullen, A.F. White, C.W. Childs, D.V. Vivit, M.S. Schulz, Demonstration of significant abiotic iron isotope fractionation in nature, Geology 29 (2001) 699–702.

[23] A.D. Anbar, J.E. Roe, J. Barling, K.H. Nealson, Nonbiological fractionation of iron isotopes, Science 288 (2000) 126–128.

[24] L.-H. Chan, M. Kastner, Lithium isotopic compositions of pore fluids and sediments in the Costa Rica subduction zone: implications for fluid processes and sediment contribution to arc volcanoes, Earth Planet. Sci. Lett. 183 (2000) 275–290.

[25] J. Barling, A.D. Anbar, Molybdenum isotope fractionation during adsorption by manganese oxides, Earth Planet. Sci. Lett. 217 (2004) 315–329.

[26] C. Siebert, T.F. Nägler, F. von Blanckenburg, J.D. Kramers, Molybdenum isotope records as a potential new proxy for paleoceanography, Earth Planet. Sci. Lett. 211 (2003) 159–171.

[27] J. Barling, G.L. Arnold, A.D. Anbar, Natural mass-dependent variations in the isotopic composition of molybdenum, Earth Planet. Sci. Lett. 193 (2001) 447–457.

[28] A.D. Matthews, J.P. Riley, The occurrence of thallium in sea water and marine sediments, Chem. Geol. 149 (1970) 149–152.

[29] A.D. Matthews, J.P. Riley, The determination of thallium

in silicate rocks, marine sediments and sea water, Anal. Chim. Acta 48 (1969) 25–34.
[30] H. Heinrichs, B. Schulz-Dobrick, K.H. Wedepohl, Terrestrial geochemistry of Cd, Bi, Tl, Pb, Zn, and Rb, Geochim. Cosmochim. Acta 44 (1980) 1519–1533.
[31] K.H. Wedepohl, Handbook of Geochemistry, Springer, Berlin, 1974.
[32] J.R. Hein, H.-W. Yeh, S.H. Gunn, W.V. Sliter, L.M. Benninger, C.-H. Wang, Two major Cenozoic episodes of phosphogenesis recorded in equatorial Pacific seamount deposits, Paleoceanography 8 (1993) 293–311.
[33] A. Koschinsky, A. Stascheit, M. Bau, P. Halbach, Effects of phospatization on the geochemical and mineralogical composition of marine ferromanganese crusts, Geochim. Cosmochim. Acta 61 (1997) 4079–4094.
[34] G.M. Henderson, K.W. Burton, Using ($^{234}U/^{238}U$) to assess diffusion rates of isotope tracers in ferromanganese crusts, Earth Planet. Sci. Lett. 170 (1999) 166–179.
[35] J.R. Hein, C.L. Morgan, Influence of substrate rocks on Fe–Mn crust composition, Deep-Sea Res. I 46 (1999) 855–875.
[36] B. Peucker-Ehrenbrink, G. Ravizza, The marine osmium isotope record, Terra Nova 12 (2000) 205–219.
[37] K.W. Bruland, Trace elements in sea-water, in: J.P. Ripley, R. Chester (Eds.), Chemical Oceanography 8, Academic Press, London, 1983, pp. 157–220.
[38] M.R. Palmer, H. Elderfield, Sr isotope composition of sea water over the past 75 Myr, Nature 314 (1985) 526–528.
[39] C.H. Lear, H. Elderfield, P.A. Wilson, Cenozoic deep-sea temperatures and global ice volumes from Mg/Ca in benthic foraminiferal calcite, Science 287 (2000) 269–272.
[40] P.N. Pearson, M.R. Palmer, Atmospheric carbon dioxide concentrations over the past 60 million years, Nature 406 (2000) 695–699.
[41] D. Lemarchand, J. Gaillardet, E. Lewin, C.J. Allègre, The influence of rivers on marine boron isotopes and implications for reconstructing past ocean pH, Nature 408 (2000) 951–954.
[42] J.P. Kennett, Marine Geology, Prentice-Hall, Englewood Cliffs, NJ, 1982, 813 pp.
[43] D.B. Rowley, Rate of plate creation and destruction: 180 Ma to present, Geol. Soc. Am. Bull. 114 (2002) 927–933.
[44] D.K. Rea, The paleoclimatic record provided by eolian deposition in the deep sea: the geological history of wind, Rev. Geophys. 32 (1994) 159–195.
[45] C.H. Lear, H. Elderfield, P.A. Wilson, A Cenozoic seawater Sr/Ca record from benthic foraminiferal calcite and its application in determining global weathering rates, Earth Planet. Sci. Lett. 208 (2003) 69–84.
[46] K.H. Freeman, J.M. Hayes, Fractionation of carbon isotopes by phytoplankton and estimates of ancient CO_2 levels, Global Biogeochem. Cycles 6 (1992) 185–198.
[47] R.A. Berner, A.C. Lasaga, R.M. Garrels, The carbonate-silicate geochemical cycle and its effect on atmospheric carbon dioxide over the past 100 million years, Am. J. Sci. 283 (1983) 641–683.
[48] D.M. Kerrick, Present and past nonanthropogenic CO_2 degassing from the solid Earth, Rev. Geophys. 39 (2001) 565–585.
[49] K. Wallmann, Controls on the Cretaceous and Cenozoic evolution of seawater composition, atmospheric CO_2 and climate, Geochim. Cosmochim. Acta 65 (2001) 3005–3025.
[50] K. Rubin, Degassing of metals and metalloids from erupting seamounts and mid-ocean ridge volcanoes: Observations and predictions, Geochim. Cosmochim. Acta 61 (1997) 3525–3542.
[51] J.M. McArthur, R.J. Howarth, T.R. Bailey, Strontium isotope stratigraphy: LOWESS version 3: Best fit to the marine Sr-isotope curve for 0–509 Ma and accompanying look-up table for deriving numerical age, J. Geol. 109 (2001) 155–170.